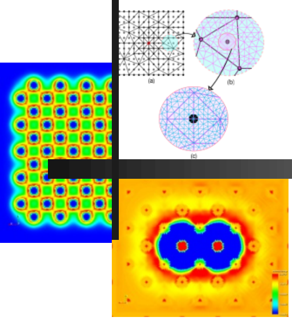

Large-scale real-space electronic structure calculations

Vikram Gavini

Department of Mechanical Engineering

University of Michigan, Ann Arbor

Collaborators: Phani Motamarri (U. Mich); Bikash Kanungo (U. Mich)

Funding: TRI, ARO, NSF, DoE-BES, XSEDE

Defective Crystals

- Defects play a crucial role in influencing a variety of materials properties – mechanical, electronic, optical, chemical
- Dislocations

Vacancies/Interstitials

Interfaces/Surfaces

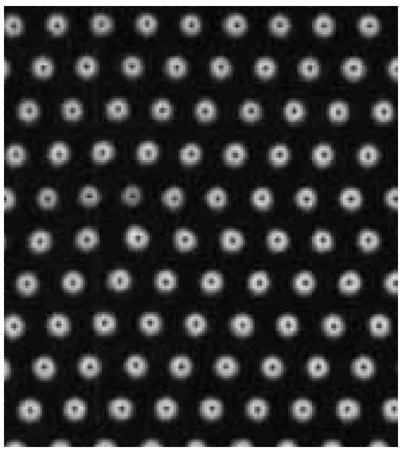

TEM image of dislocation partial
T.J. Balk, K.J. Hemker, Phil. Mag. A, 2001

Metal Plasticity – Renders the strength of materials to 1/1000 its theoretical strength

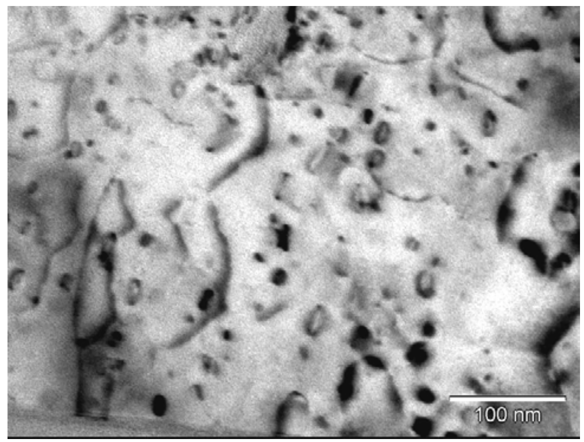

Prismatic loops formed from vacancies,
Giess et. al, Microsc Microanal, 2005

Creep, Spall, Ageing, hardening due to radiation

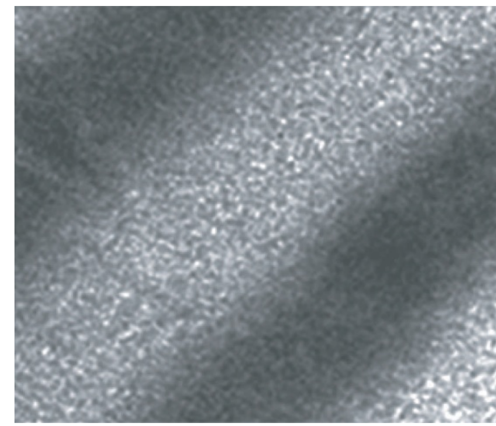

TEM image of Ni-Al interface,
Mann et.al, J. Appl. Phys. 1997

Phase stability, Energetics, Diffusion mediation, defect sources and sinks

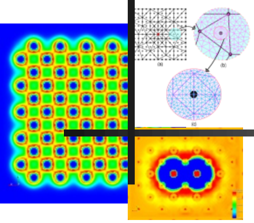

Defective crystals: The challenge

- The energetics of defects: (i) core-energy; (ii) elastic energy
- The core of a defect is governed by electronic structure – need electronic structure calculations!
- Defects result in a vast span of *interacting* length scales
  - Electronic structure of the core (10^{-12} m)
  - Complex rearrangements of atoms around the core (10^{-9} m)
  - Long ranged elastic effects (10^{-6} m)

But need single physics at all length scales! - No patching, seamless description

Realistic defect concentration in materials is parts per million!

- Challenge : Need electronic structure calculations at macroscopic scales!
  - (i) Development of computational techniques for large-scale electronic structure calculation that can explicitly treat systems up to 10,000 atoms
  - (ii) Development of seamless coarse-graining schemes using adaptive numerical schemes

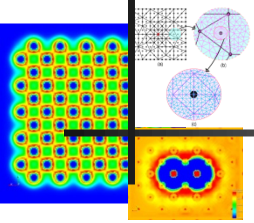

Quantum Mechanics

- Schrödinger equation - $H\psi = E\psi$

$$H = -\frac{1}{2}\sum_{i=1}^{N}\nabla_i^2 - \frac{1}{2}\sum_{A=1}^{M}\frac{1}{M_A}\nabla_A^2 - \sum_{i=1}^{N}\sum_{A=1}^{M}\frac{Z_A}{|\mathbf{r}_i - \mathbf{R}_A|} + \sum_{i=1}^{N}\sum_{j>i}^{N}\frac{1}{|\mathbf{r}_i - \mathbf{r}_j|} + \sum_{A=1}^{M}\sum_{B=1,B>A}^{M}\frac{Z_A Z_B}{|\mathbf{R}_A - \mathbf{R}_B|}$$

$$\psi = \psi(\mathbf{x}_1, \mathbf{x}_2, ..., \mathbf{x}_N, \mathbf{R}_1, \mathbf{R}_2, ..., \mathbf{R}_M)$$

- Born-Oppenheimer approximation - Classical treatment of atomic nuclei

$$\psi = \psi(\mathbf{x}_1, \mathbf{x}_2, ..., \mathbf{x}_N)$$

- Computational complexity - $\psi \in \mathbf{R}^{3N}$!!

Density-functional theory – Kohn-Sham approach

- Ground-state energy is a function of electron-density !! (Kohn & Sham, 1964-65)

$$\langle\psi|H|\psi\rangle \geq E_0 \qquad \text{(Variational statement)}$$

$$\begin{aligned}
E_0 &= \min_{\psi} \langle\psi|T + \frac{1}{2}\sum_i \sum_j{}' \frac{1}{|\mathbf{r}_i - \mathbf{r}_j|} + \sum_i V_{ext}(\mathbf{r}_i)|\psi\rangle + E_{zz} \\
&= \min_{\psi} \langle\psi|T + \frac{1}{2}\sum_i \sum_j{}' \frac{1}{|\mathbf{r}_i - \mathbf{r}_j|}|\psi\rangle + \int \rho(\mathbf{r}) V_{ext}(\mathbf{r}) d\mathbf{r} + E_{zz} \\
&= \min_{\rho} \left\{ \underbrace{\left(\min_{\psi\to\rho} \langle\psi|T + \frac{1}{2}\sum_i \sum_j{}' \frac{1}{|\mathbf{r}_i - \mathbf{r}_j|}|\psi\rangle \right)}_{F(\rho)} + \int \rho(\mathbf{r}) V_{ext}(\mathbf{r}) d\mathbf{r} \right\} + E_{zz}
\end{aligned}$$

$$F(\rho) = T_s(\rho) + E_H(\rho) + E_{xc}(\rho)$$

$\longrightarrow$ Exchange-correlation functional: Model using LDA, GGA

$T_s(\rho)$ $\downarrow$ Kinetic energy of non-interacting electrons: Computed from wave-functions of the resulting E-L eqn.

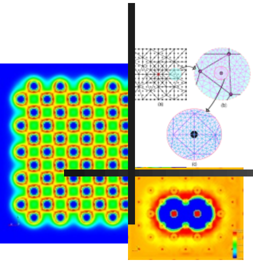

Kohn-Sham density-functional theory (KSDFT)

- The KSDFT energy functional is given by,

$$E(\Psi,\mathbf{R}) = T_s(\Psi) + E_{xc}(\rho) + E_H(\rho) + E_{ext}(\rho,\mathbf{R}) + E_{ZZ}(\mathbf{R})$$

$$\text{where} \quad \Psi = \left\{\psi_1(\mathbf{r}),\psi_2(\mathbf{r}),\ldots,\psi_N(\mathbf{r})\right\}$$

$$\rho(\mathbf{r}) = \sum_i |\psi_i(\mathbf{r})|^2$$

$$T_s(\Psi) = \sum_i \frac{1}{2}\int |\nabla\psi_i(\mathbf{r})|^2 d\mathbf{r}$$

$$E_{xc}(\rho) = \int \epsilon_{xc}(\rho(\mathbf{r}))\rho(\mathbf{r})d\mathbf{r};$$

Local density approximation (LDA)

Non-local

$$E_H(\rho) = \frac{1}{2}\int\int \frac{\rho(\mathbf{r})\rho(\mathbf{r}')}{|\mathbf{r}-\mathbf{r}'|}d\mathbf{r}d\mathbf{r}';$$

$$E_{ext}(\rho,\mathbf{R}) = \int \rho(\mathbf{r})V_{ext}(\mathbf{r})d\mathbf{r} = \sum_{I=1}^{M}\int \rho(\mathbf{r})\frac{Z_I}{|\mathbf{r}-\mathbf{R}_I|}d\mathbf{r}$$

$$E_{zz}(\mathbf{R}) = \frac{1}{2}\sum_{I=1}^{M}\sum_{J=1,J\neq I}^{M}\frac{Z_I Z_J}{|\mathbf{R}_I-\mathbf{R}_J|};$$

Classical electrostatic interaction energy :

Computed in Fourier-space (reciprocal-space) in almost all DFT implementations

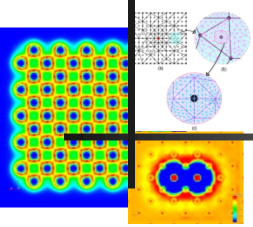

KSDFT – Real-space formulation

(Suryanarayana & Gavini et al. JMPS 58, 256-280 (2010))

Non-local

$$E_H(\rho) = \frac{1}{2}\int\int \frac{\rho(\mathbf{r})\rho(\mathbf{r}')}{|\mathbf{r}-\mathbf{r}'|}d\mathbf{r}d\mathbf{r}';$$

$$E_{ext}(\rho,\mathbf{R}) = \sum_{I=1}^{M}\int \frac{\rho(\mathbf{r})Z_I}{|\mathbf{r}-\mathbf{R}_I|}d\mathbf{r};$$

$$E_{zz}(\mathbf{R}) = \frac{1}{2}\sum_{I=1}^{M}\sum_{J=1,J\neq I}^{M}\frac{Z_I Z_J}{|\mathbf{R}_I-\mathbf{R}_J|};$$

$\frac{1}{|\mathbf{r}-\mathbf{r}'|} \longrightarrow$ Green's function for Laplace operator

- Electrostatic interactions can be re-written locally as,

$$E_H(\rho) + E_{ext}(\rho,\mathbf{R}) + E_{ZZ}(\mathbf{R}) =$$

$$-\inf_{\phi\in H^1(\mathbb{R}^3)}\left\{\frac{1}{8\pi}\int|\nabla\phi(\mathbf{r})|^2 d\mathbf{r} - \int(\rho(\mathbf{r})+b(\mathbf{r};\mathbf{R}))\phi(\mathbf{r})d\mathbf{r}\right\}$$

(Regularized nuclear charges)

- Thus, $E(\Psi,\mathbf{R}) = \sup_{\phi\in H^1(\mathbb{R}^3)} L(\Psi,\mathbf{R},\phi)$

$$L(\Psi,\mathbf{R},\phi) = \sum_i \frac{1}{2}\int|\nabla\psi_i(\mathbf{r})|^2 d\mathbf{r} + \int\epsilon_{xc}(\rho(\mathbf{r}))\rho(\mathbf{r})d\mathbf{r}$$
$$-\frac{1}{8\pi}\int|\nabla\phi(\mathbf{r})|^2 d\mathbf{r} + \int(\rho(\mathbf{r})+b(\mathbf{r}))\phi(\mathbf{r})d\mathbf{r}$$

KSDFT – Real-space formulation

(Suryanarayana & Gavini et al. JMPS 58, 256-280 (2010))

- The saddle-point problem is given by,

$$\inf_{\mathbf{R}\in\mathbf{R}^{3M}} \inf_{\Psi\in X} \sup_{\phi\in H^1(\mathbb{R}^3)} L(\Psi,\mathbf{R},\phi)$$

$$\begin{aligned} L(\Psi,\mathbf{R},\phi) \quad &= \quad \sum_i \frac{1}{2}\int |\nabla\psi_i(\mathbf{r})|^2 d\mathbf{r} + \int \epsilon_{xc}(\rho(\mathbf{r}))\rho(\mathbf{r})d\mathbf{r} \\ &\quad -\frac{1}{8\pi}\int |\nabla\phi(\mathbf{r})|^2 d\mathbf{r} + \int (\rho(\mathbf{r})+b(\mathbf{r}))\phi(\mathbf{r})d\mathbf{r} \end{aligned}$$

- Define, $X = \left\{\Psi | \Psi \in (H_0^1(\Omega))^N, \langle\psi_i,\psi_j\rangle = \delta_{ij}\right\}$

- Theorem : $E(\Psi)$ has a minimum in X.

  Proof : Sobolev embeddings; Poincaré inequality (Direct Method)

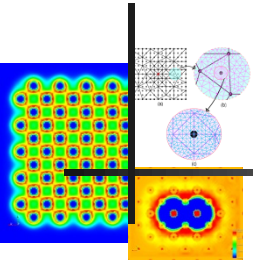

Kohn-Sham eigenvalue problem

- $$E_0(\mathbf{R}) = \min_{\Psi \in X} E(\Psi, \mathbf{R}) = \min_{\Psi \in X} \max_{\phi \in H^1(\mathbb{R}^3)} L(\Psi, \mathbf{R}, \phi)$$

- Consider the E-L equation corresponding to the variational problem:

$$\left(-\frac{1}{2}\nabla^2 + V_{eff}\right)\psi_i = \epsilon_i \psi_i$$

Self consistent iteration
(Kohn-Sham map)

$$\rho = \sum_i f_i |\psi_i|^2, \qquad V_{eff}(\mathbf{r}) = V_H(\rho(\mathbf{r})) + V_{xc}(\rho(\mathbf{r})) + V_{ext}(\mathbf{R})$$

$$T_s(\Psi) = \frac{1}{2}\sum_i f_i \int |\nabla \psi_i(\mathbf{r})|^2 d\mathbf{r} \quad E_0(\Psi) = T_s(\Psi) + E_{xc}(\rho) + E_H(\rho) + E_{ext}(\rho) + E_{zz}$$

- To avoid charge-sloshing:

$$f_i = f(\varepsilon_i, \mu) = \frac{1}{1 + e^{\frac{\varepsilon_i - \mu}{k_B T}}} \qquad \sum_i f_i = N$$

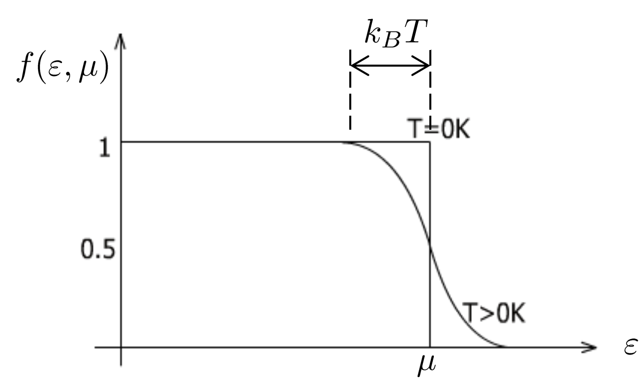

State of the art

Solutions to Kohn-Sham Equations

Fourier Space Formulations

Real Space Formulations (LCAO, FDM, FEM)

<u>Key Features (plane-waves)</u>

- Very efficient for periodic calculations
- Restrictive to periodic domains
- Provide only uniform spatial resolution
- Suitable only when the solution fields are smooth.

<u>Key Features (LCAO)</u>

- Suitable for isolated systems
- Can handle both pseudopotential and all electron calculations
- Systematic convergence can not be ascertained
- Parallel scalability is a concern

KSDFT – FE discretization

- Use finite-element basis for computing –

$$\psi_k^h(\mathbf{r}) = \sum_i \psi_{k\,i} N_i(\mathbf{r}) \;\; k = 1, \ldots, N\,, \qquad \phi^h(\mathbf{r}) = \sum_i \phi_i N_i(\mathbf{r})$$

ψ_{k_i}, ϕ_i … – Nodal values
$N_i(\mathbf{r})$ – Shape functions

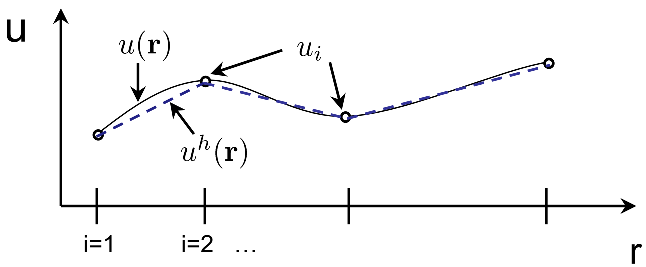

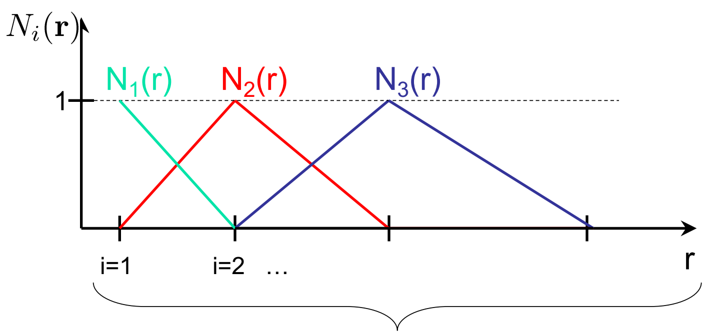

By changing the positioning of the nodes the spatial resolution of basis can be changed/adapted

Features of finite-element basis:

1. Unstructured coarse-graining
2. Complex geometries can be represented, and arbitrary boundary conditions can be imposed.
3. Systematic convergence
4. Ease of parallel implementation

KSDFT – FE discretization

Main Limitations:

- Previous attempts showed that the number of FE basis functions (linear) needed to obtain chemical accuracy is very large ~ 100,000-1,000,000 basis functions per atom.

- The finite-element discretization leads to a generalized eigenvalue problem, which is more challenging to solve than a standard eigenvalue problem

Present Work:

- We demonstrate an efficient, scalable computational approach using adaptive higher-order finite-element discretization.

- We propose a linear scaling algorithm (in number of electrons) which treats both insulating and metallic systems on an equal footing.

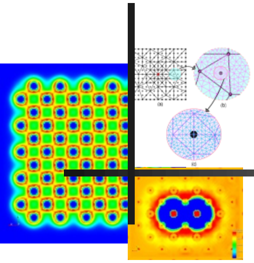

KSDFT – FE discretization

- Discrete eigenvalue problem:

$$\mathbf{H}\hat{\psi}_k = \varepsilon_k^h \mathbf{M}\hat{\psi}_k$$

$$\begin{aligned}
\mathbf{H}_{ij} &= \frac{1}{2}\int_\Omega \nabla N_i(\mathbf{r}).\nabla N_j(\mathbf{r})d\mathbf{r} + \int_\Omega V_{eff}(\mathbf{r},\mathbf{R})N_i(\mathbf{r})N_j(\mathbf{r})d\mathbf{r} \\
\mathbf{M}_{ij} &= \int_\Omega N_i(\mathbf{r})N_j(\mathbf{r})d\mathbf{r}
\end{aligned}$$

- Transformation to a standard eigenvalue problem:

$$\tilde{\mathbf{H}}\tilde{\psi}_k = \varepsilon_k^h\tilde{\psi}_k \quad \text{where} \quad \tilde{\mathbf{H}} = \mathbf{M}^{-1/2}\mathbf{H}\mathbf{M}^{-1/2} \quad \text{and} \quad \tilde{\psi}_k = \mathbf{M}^{1/2}\hat{\psi}_k$$

- Remark: $\tilde{\mathbf{H}}$ denotes the projection of the Hamiltonian operator into a space spanned by Löwden orthonormalized finite-element basis

Can higher-order finite-elements do any better?

- Here, we investigate the viability and computational efficiency afforded by higher-order finite-element discretization in electronic structure calculations using density functional theory to answer the following questions:
    - What is the numerical convergence rate for various orders of finite-element approximations in electronic structure calculations using DFT?
    - What is the computational advantage derived by using higher-order finite element discretization in terms of the CPU time?
- First studies which demonstrate the computational efficiency afforded by higher-order elements for Kohn-Sham DFT calculations.

Rate of convergence of the finite element approximation

- The study has been carried out by a suite of higher order elements:
  - TET 10 (TETRAHEDRAL QUADRATIC ELEMENT)
  - HEX 27 (TRI QUADRATIC HEXAHEDRAL ELEMENT)
  - HEX 64 (TRI CUBIC HEXAHEDRAL ELEMENT)
  - HEX 125 (TRI QUARTIC HEXAHEDRAL ELEMENT)
  - HEX 64 SPECTRAL, HEX 125 SPECTRAL … upto 10th order

  (Lagrange Polynomials are constructed on Gauss-Lobatto Legendre Points for spectral elements)

- Elements have been tested against three types of problems: (a) CH_4 (b) Barium Cluster (35 atoms)

  (a) CH_4 : An all electron calculation
  (b) Barium Cluster: Pseudopotential calculation

Convergence rates

(Motamarri et al. J. Comp. Phys. 253, 308-343 (2013))

Barium Cluster

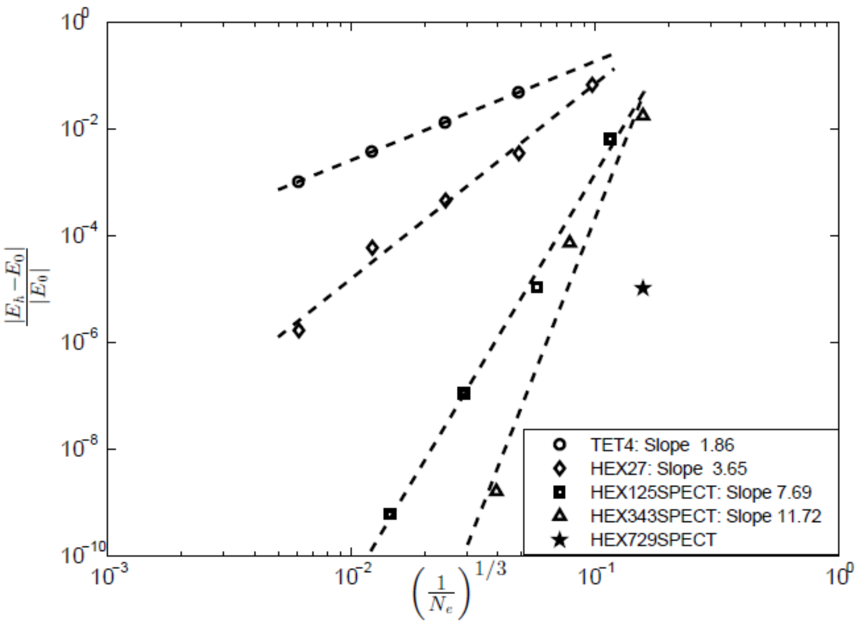

Methane Molecule

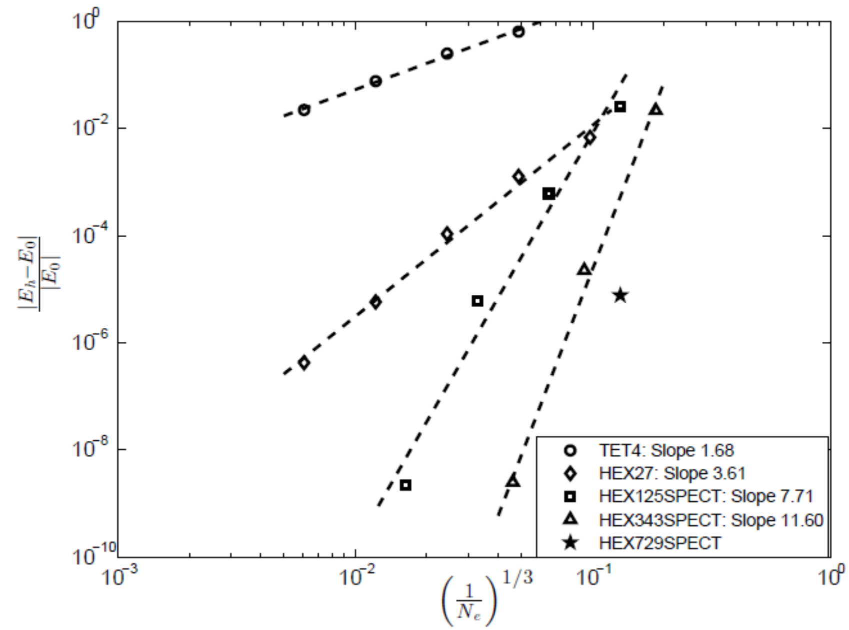

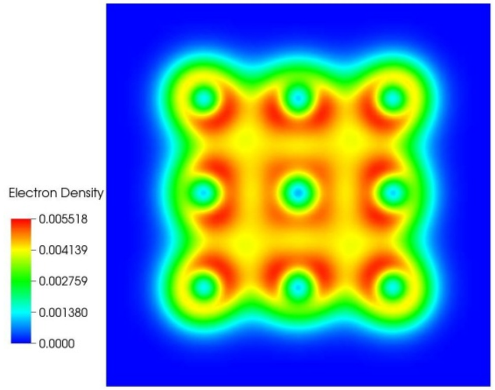

Optimal rate of convergence!

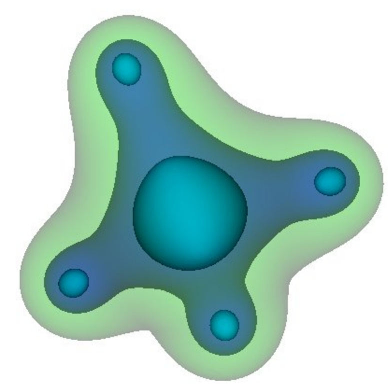

Computational efficiency of higher-order FE discretization

Two Key questions:

- How do higher-order FE discretizations compare to lower order elements in computational efficiency?
- How do higher-order FE discretizations compare against plane-wave basis and Gaussian basis?

Key ideas in improving computational efficiency:

- Developed *a priori* mesh adaption techniques
- Use of Gauss-Legendre-Lobatto quadrature rules for the overlap matrix in conjunction with Spectral FE discretization
- Developed a Chebyschev acceleration technique to directly compute the eigenspace

A priori mesh adaption

(Motamarri et al. J. Comp. Phys. 253, 308-343 (2013))

Error Estimate:

$$|E-E_h| \leq C\left(\sum_i ||\psi_i - \psi_i^h||^2_{1,\Omega} + |\phi - \phi^h|^2_{1,\Omega} + \sum_i ||\psi_i - \psi_i^h||_{0,\Omega}||\phi - \phi^h||_{1,\Omega}\right)$$

$$\Downarrow$$

$$\begin{aligned} |E-E_h| &\leq C\sum_{e=1}^{N_e}\int_{\Omega_e}\left(h_e^{2k}\left[\sum_i |D^{k+1}\psi_i(\mathbf{r})|^2 + |D^{k+1}\phi(\mathbf{r})|^2\right]d\mathbf{r}\right) \\ &\leq C'\int_{\Omega}\left(h^{2k}(\mathbf{r})\left[\sum_i |D^{k+1}\psi_i(\mathbf{r})|^2 + |D^{k+1}\phi(\mathbf{r})|^2\right]d\mathbf{r}\right) \end{aligned}$$

Optimal mesh distribution:

$$\min_h \; |E-E_h| \qquad \text{subject to: } \int_\Omega \frac{d\mathbf{r}}{h^3(\mathbf{r})} = N_e$$

Spectral FE and Gauss-Lobatto-Legendre quadrature

- *Spectral-element basis functions:*

  - Constructed from Lagrange polynomials interpolated through nodes corresponding to the roots of the derivatives of the Legendre polynomials and boundary nodes (GLL points)

  - Upon using a Gauss-Lobatto-Legendre quadrature rule, the quadrature points coincide with the FE nodes

$$\mathbf{M}_{ij} = \int_{\Omega_e} N_i(\mathbf{r}) N_j(\mathbf{r}) d\mathbf{r} = C_i \delta_{ij}$$

- *Remarks:*
  - Transformation to standard eigenvalue problem is trivial

  - The reduced order quadrature rule is only employed for the computation of the overlap matrix, and the full Gauss quadrature is employed to compute the Hamiltonian matrix.

Eigen-space computation: Chebyschev acceleration

(Motamarri et al. J. Comp. Phys. 253, 308-343 (2013))

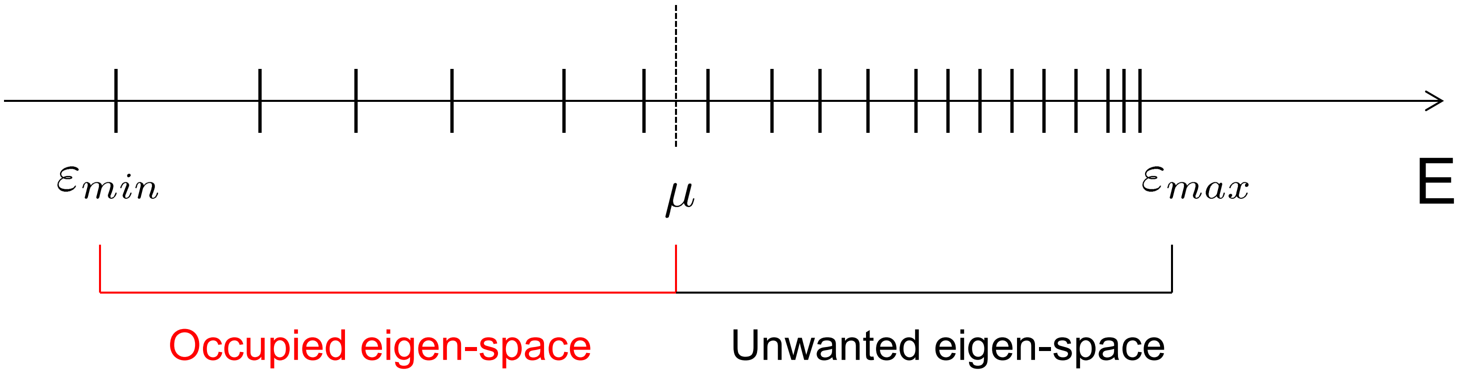

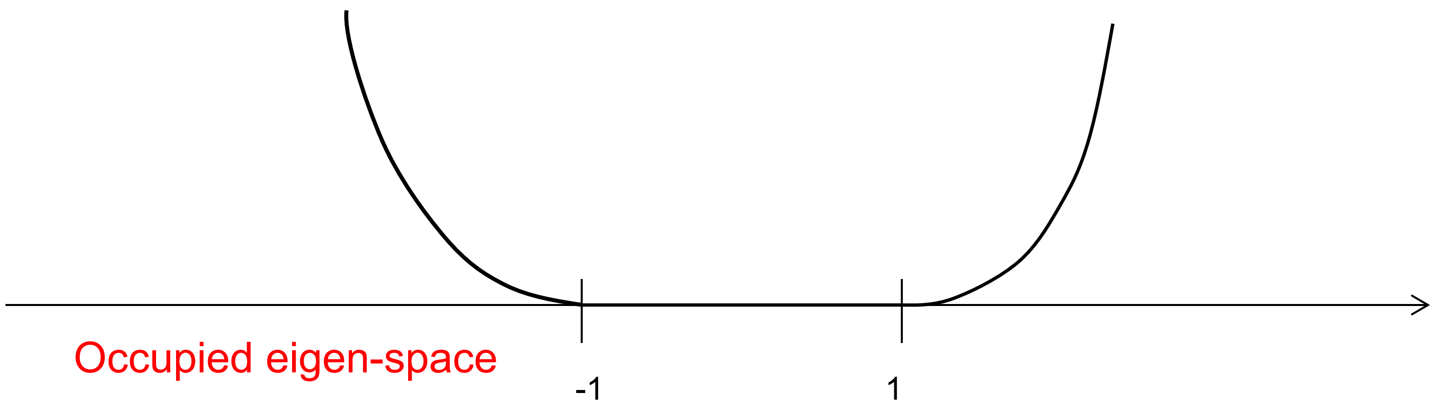

$$\overline{\mathbf{H}} = c_1 \tilde{\mathbf{H}} + c_2$$

Eigen-space computation: Chebyschev acceleration

Table 1: Comparison of Generalized vs Standard eigenvalue problems.

Element Type	DOFs	Problem Type	N	Time (GHEP)	Time (SHEP)
HEX125SPECT	1,368,801	graphene	96	1786 CPU-hrs	150 CPU-hrs
HEX343SPECT	2,808,385	Al $3 \times 3 \times 3$ cluster	516	2084 CPU-hrs	80 CPU-hrs

Table 2: Comparison of Standard eigenvalue problem vs Chebyshev filtered subspace iteration (ChFSI).

Element Type	DOFs	Problem Type	N	Time (SHEP)	Time (ChFSI)
HEX125SPECT	1,368,801	graphene	96	150 CPU-hrs	12.5 CPU-hrs
HEX343SPECT	2,808,385	Al $3 \times 3 \times 3$ cluster	512	80 CPU-hrs	13 CPU-hrs

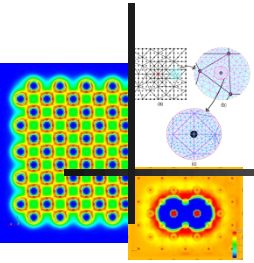

Numerical algorithm

1. Start with initial guess for electron density $\rho_{in}^{h}(\mathbf{r}) = \rho_0(\mathbf{r})$ and the initial wavefunctions $\Psi = \{\tilde{\psi}_1 \ldots \tilde{\psi}_{\bar{N}}\}$
2. Compute the discrete Hamiltonian $\overline{\mathbf{H}}$ using the input electron density ρ_{in}^{h}
3. Compute the Chebyshev filtered basis : $\Phi = T_m(\overline{\mathbf{H}})\Psi$
4. Orthonormalize the basis Φ and compute $\overline{\mathbf{H}}^{\Phi} = \Phi^T \overline{\mathbf{H}} \Phi$, the projected Hamiltonian into the subspace spanned by Φ
5. Compute the Fermi-energy and the output electron density by diagonalizing projected Hamiltonian and using the following equation

$$\rho_{out}^{h}(\mathbf{r}) = \sum_i f(\varepsilon_i, \mu) |\psi_i^h(\mathbf{r})| \quad \text{where} \quad f(\varepsilon_i, \mu) = \frac{1}{1 + e^{\frac{\varepsilon_i - \mu}{k_B T}}}$$

6. If $||\rho_{out}^{h}(\mathbf{r}) - \rho_{in}^{h}(\mathbf{r})|| < tol$, EXIT; else, compute new ρ_{in}^{h} using a mixing scheme and go to (2).

Computational efficiency

(Motamarri et al. J. Comp. Phys. 253, 308-343 (2013))

Barium Cluster

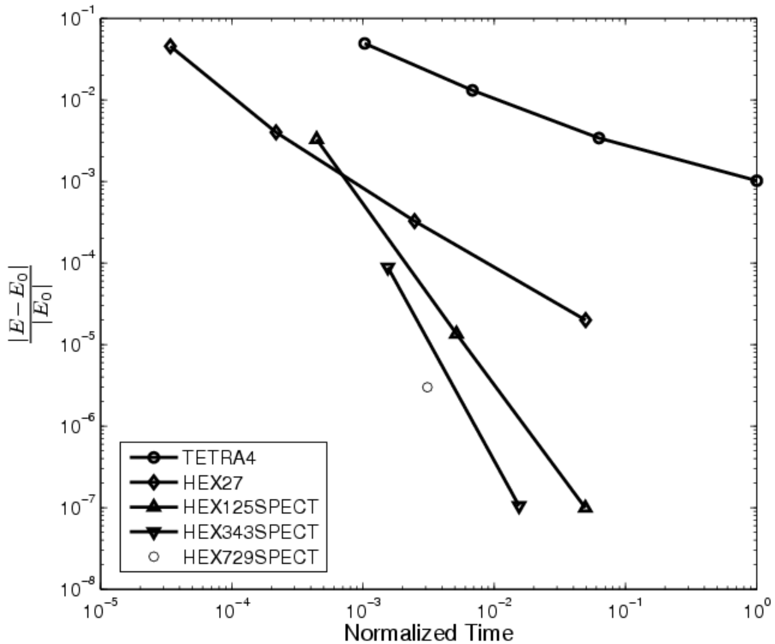

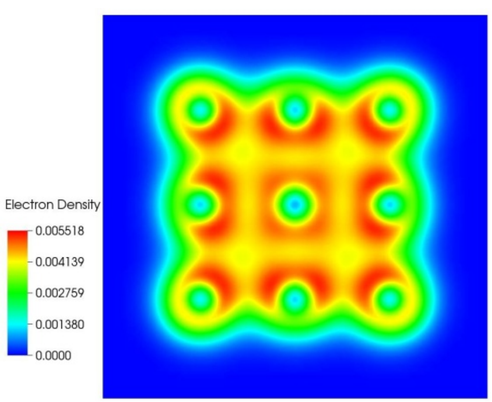

Methane Molecule

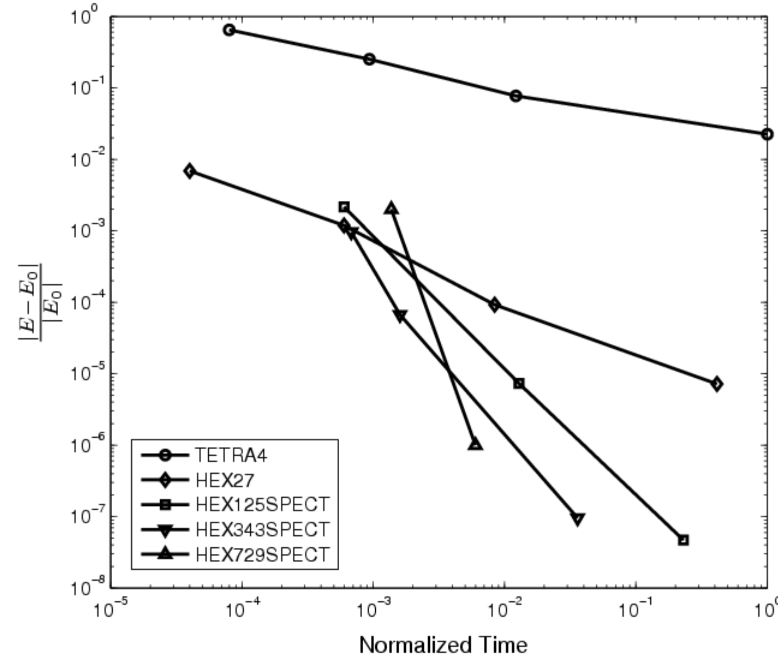

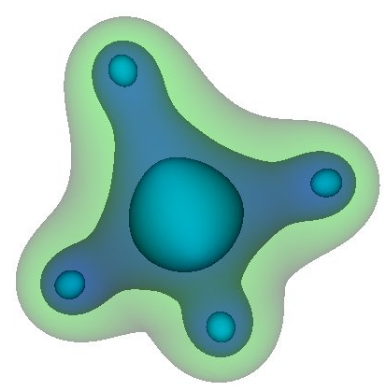

Aluminum clusters

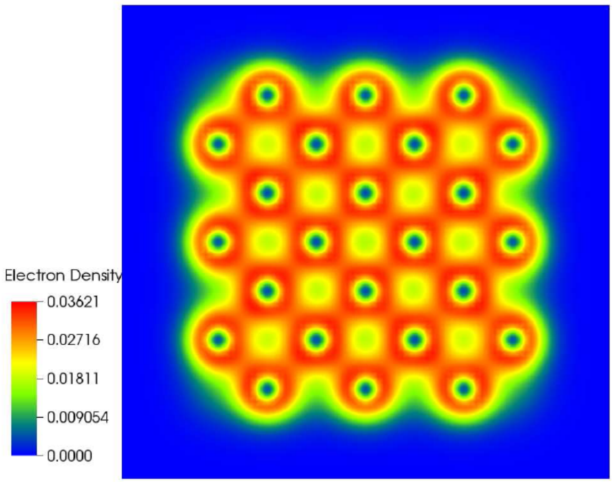

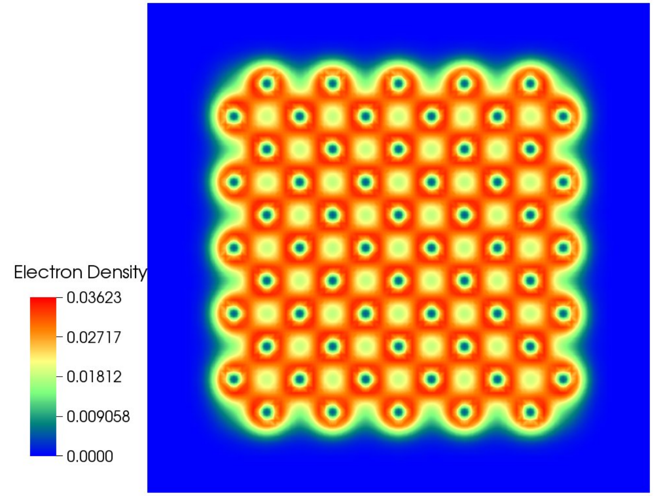

Type of basis set	**Energy per atom** (eV)	**Abs. error** $(meV/atom)$	**CPU Hrs**
Plane-waves (20 Ha; 60 $a.u.$; $461,165$ basis)	-56.69289	3.8	910
FE basis (5th order; $1,107,471$ nodes)	-56.69497	2.0	147

Type of basis set	**Energy per atom** (eV)	**Abs. error** $(meV/atom)$	**CPU Hrs**
Plane-waves (20 Ha; 80 $a.u.$; $1,093,421$ basis)	-56.87392	4.3	8640
FE basis (5th order; $4,363,621$ nodes)	-56.87652	2.1	1132

Scalability

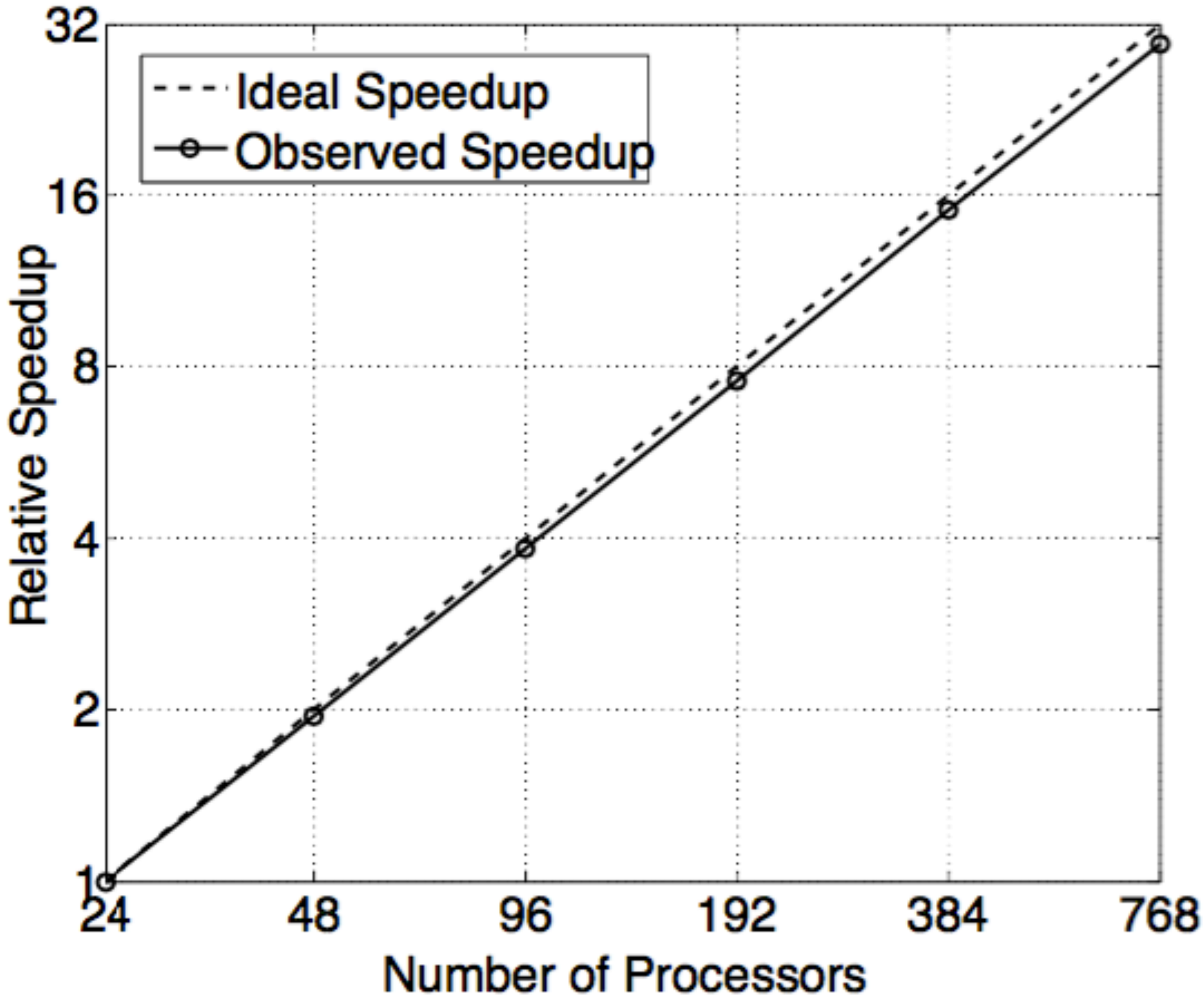

All-electron calculations

100 atom Graphene sheet

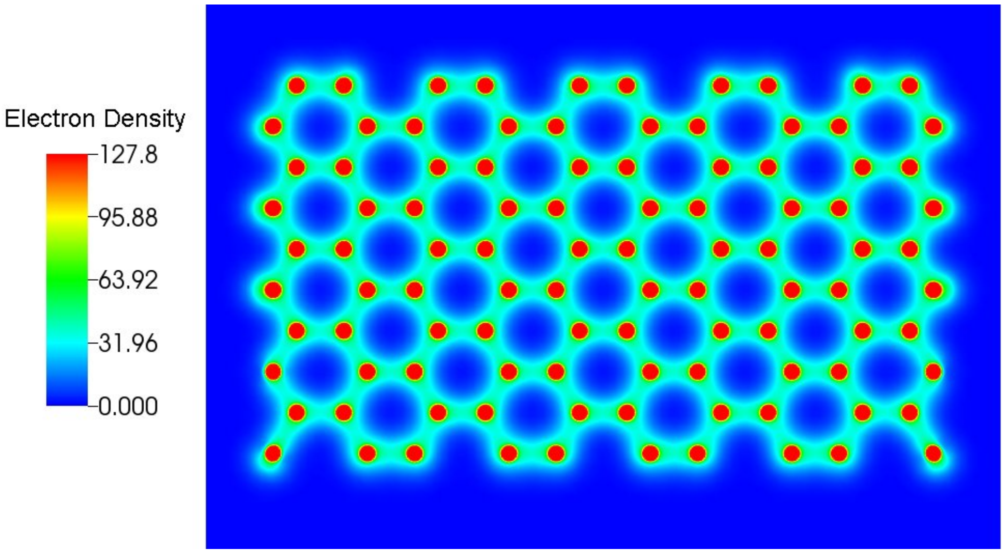

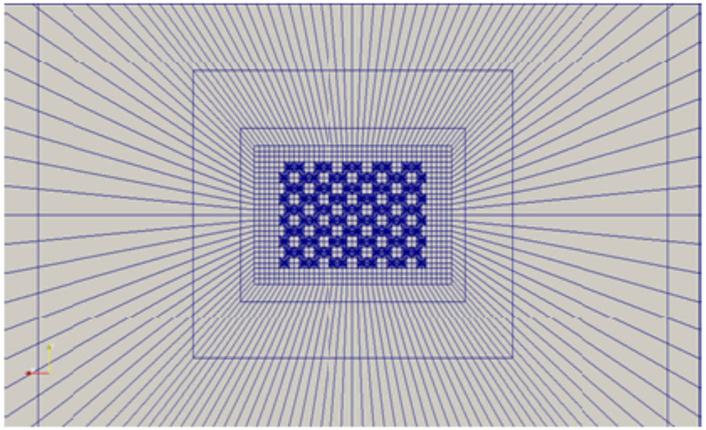

Type of basis set	Relative error	Time (CPU-hrs)
pc2 (Gaussian, $3,000$ basis functions)	1.06×10^{-4}	666
FE basis (HEX125SPECT, $8,004,003$ nodes)	1.2×10^{-4}	7461

Enriched FE basis

(Kanungo & Gavini Phys. Rev. B 95, 035112 (2017))

- Additional functions appended to the 'Classical' FE basis

$$\psi^h(\mathbf{x}) = \sum_j N_j^C(\mathbf{x})\psi_j^C + \sum_k N_k^E(\mathbf{x})\psi_j^E$$

- Enriched functions: Radial part computed using 1D radial Kohn-Sham solve, and multiplied by spherical harmonics

- Compact support for the enriched functions is obtained by multiplying with a mollifier

- Integrals computed using an adaptive quadrature (Mousavi et al. (2012))

- Key advantages of enrichment:
  - Reduced degrees of freedom
  - Reduced spectral width of the discrete Hamiltonian

Enriched FE basis

$$M = \left[\begin{array}{c|c} M_{11} & M_{21}^T \\ \hline M_{21} & M_{22} \end{array}\right] \qquad M^{-1} = \left[\begin{array}{c|c} M_{11}^{-1} + L^T S^{-1} L & -L^T S^{-1} \\ \hline -S^{-1} L & S^{-1} \end{array}\right]$$

$$L = M_{21} M_{11}^{-1} \qquad S = M_{22} - M_{21} M_{11}^{-1} M_{21}^T$$

- M_{11} is diagonal when spectral FE are used along with Guass-Lobatto quadrature
- S is a small matrix of size N_{el} x N_{el} and can be easily inverted using direct solvers

Enriched FE basis v/s Classical FE basis

Silicon 1x1x1: 18 atoms (252 electrons)

FE Type	Energy per atom (Ha)	# Basis functions per atom	Chebyshev Degree	CPU Hrs
EFEM	-288.31935809	27261	80	42.60
CFEM	-288.32003559	402112	1500	1599.15

Silicon 2x1x1: 31 atoms (434 electrons)

FE Type	Energy per atom (Ha)	# Basis functions per atom	Chebyshev Degree	CPU Hrs
EFEM	-288.33338251	25368	80	139.97
CFEM	-288.33412399	386205	1500	16441.43

Silicon 2x2x2: 95 atoms (1330 electrons)

FE Type	Energy per atom (Ha)	# Basis functions per atom	Chebyshev Degree	CPU Hrs
EFEM	-288.35939776	20074	80	1076.46
CFEM	-288.35945954	360467	1500	75936.4

Enriched FE basis v/s pc basis (NWChem)

Silicon 1x1x1: 18 atoms (252 electrons)

Basis	Energy per atom (*Ha*)	CPU Hrs
EFEM	−288.3193580	42.60
pc-3	−288.31899656	12.21
pc-4	−288.31944856	98.88

Silicon 2x1x1: 31 atoms (434 electrons)

Basis	Energy per atom (*Ha*)	CPU Hrs
EFEM	−288.333382	139.97
pc-3	−288.3334470	261.69
pc-4	−288.3338987	3580.08

Silicon 2x2x2: 95 atoms (1330 electrons)

Basis	Energy per atom (*Ha*)	CPU Hrs
EFEM	−288.3593977	1076.46
pc-3	−288.36004547	4097.29
pc-4	Didn't Converge	N/A

Enriched FE basis v/s pc basis (NWChem)

Silicon 3x3x3: 280 atoms (3920 electrons)

Basis	**Energy per atom** (Ha)	**CPU Hrs**
EFEM	-288.37247084	10052.78
pc-3	Didn't Converge	N/A
pc-4	Didn't Converge	N/A

Silicon 4x4x4: 621 atoms (8694 electrons)

Basis	**Energy per atom** (Ha)	**CPU Hrs**
EFEM	-288.38224514	92816.16
pc-3	Didn't Converge	N/A
pc-4	Didn't Converge	N/A

Computational complexity

Complexity in each SCF iteration:

M: Number of degrees of freedom

N: Number of electrons ($M \propto N$)

- Chebyshev filtering procedure : O(MN)
- Orthonormalization of Chebyschev filtered vectors : O(MN^2)
- Diagonalization of the projected Hamiltonian: O(N^3)

Cubic Scaling in N!

Subspace projection technique

(Motamarri & Gavini, Phys. Rev. B 90 115127 (2014))

Key features of the proposed method:

- Chebyshev filtering to generate the approximate occupied subspace
- Construct non-orthogonal localized basis functions that span the same space & truncate these localized functions beyond a prescribed tolerance
  - Subsequently localized basis functions have a compact support
  - Use an adaptive tolerance for the truncation: truncation tolerance tied to the error in the SCF iteration; ensures strict control on accuracy
- Project Hamiltonian into the occupied subspace expressed in the non-orthogonal basis
- Fermi-operator expansion of the projected Hamiltonian to estimate Fermi-energy and compute the electron density
  - Avoids diagonalization of the Hamiltonian to compute orbital occupancies
  - Applicable for both metallic and insulating systems
  - Applicable for both pseudopotenial and all-electron calculations

Subspace projection approach: Key ideas

$$\Phi = \{\psi_1, \psi_2, \psi_3, \ldots, \psi_N\} \longrightarrow$$ Eigen-space from Chebyschev filtering

$$\inf_{\psi' \in \Phi} \int w_I(\mathbf{x}) |\psi'(\mathbf{x})|^2 d\mathbf{x} \longrightarrow \Phi = \{\psi'_1, \psi'_2, \psi'_3, \ldots, \psi'_N\}$$

Localized basis spanning eigen-space
(Garcia-Cervera et al.)

- Project Hamiltonian in the localized basis:

$$\tilde{\mathbf{H}}^{\Phi} = S^{-1} \Phi_L^T \tilde{\mathbf{H}} \Phi_L \qquad S = \Phi_L^T \Phi_L$$

- Remarks:
  - Locality of $\Phi_L \implies S$ is sparse and can be computed in O(N) complexity
  - S^{-1} can be computed using Newton-Schultz algorithm which has O(N) complexity
  - Finally, $\tilde{\mathbf{H}}^{\Phi}$ can be computed in O(N), if S^{-1} is sparse.

Subspace projection approach: Key ideas

- *Computation of electron density*

Recall: $$\rho = \sum_i f_i |\psi_i|^2, \quad f_i = f(\varepsilon_i, \mu) = \frac{1}{1 + e^{\frac{\varepsilon_i - \mu}{k_B T}}}$$

No diagonalization ⇒ No knowledge of eigenvalues and eigenvectors

- *Compute density matrix instead:* $\Gamma = f(\tilde{\mathbf{H}} - \mu \mathbf{I})$
  - The electron density is the diagonal of the density matrix

- Fermi-operator expansion techniques can be employed to compute the density matrix:

$$f(\tilde{\mathbf{H}} - \mu \mathbf{I}) \approx \sum_{n=1}^{P} c_n T_n(\tilde{\mathbf{H}})$$

- Challenge: $P \sim O(\frac{\varepsilon_{max} - \varepsilon_{min}}{k_B T})$; spectral width of the discrete Hamiltonian is about 10^3 – 10^6 !

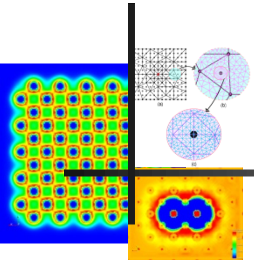

Subspace projection approach: Key ideas

Fermi-operator expansion of the projected Hamiltonian:

- Compute the density matrix using the projected Hamiltonian in the non-orthogonal localized basis

$$\Gamma = \Phi_L f(\tilde{\mathbf{H}}^{\Phi} - \mu \mathbf{I}) S^{-1} \Phi_L^T$$

- The spectral width of the projected Hamiltonian is ~ O(10) and thus can efficiently employ the Fermi-operator expansion
  - This approach treats both insulating and metallic systems on equal footing
  - This approach is applicable for both pseudopotential calculations and all-electron calculations

Case study: Al nano-clusters (3x3x3 – 9x9x9)
Pseudopotential calculations

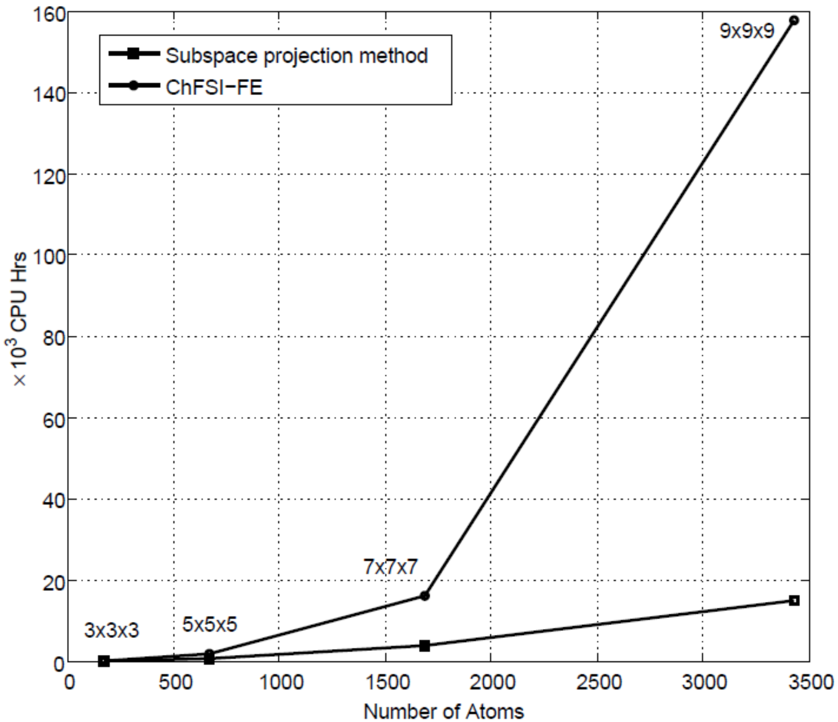

Total computational time

Subspace projection scaling: $O(N^{1.46})$

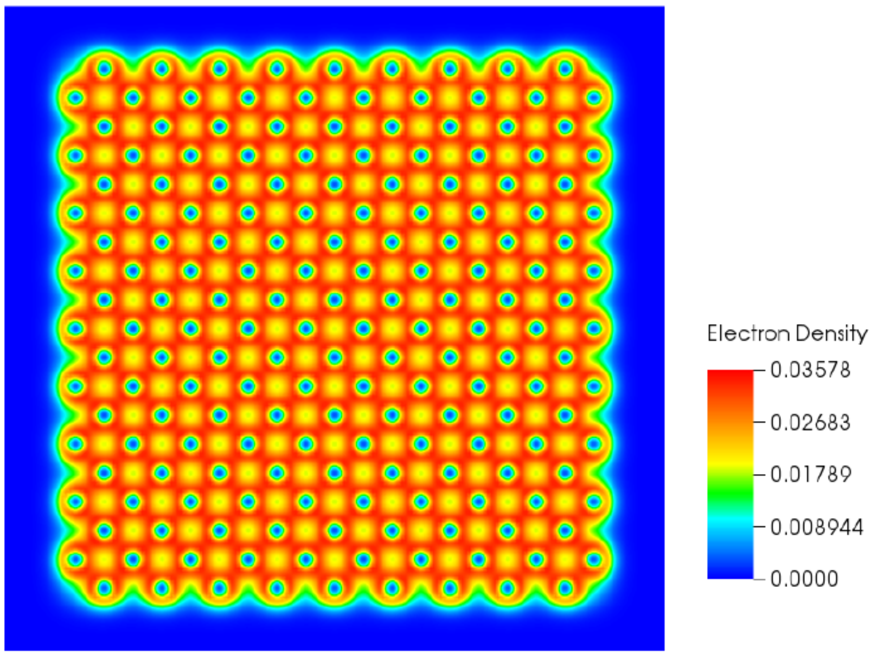

Electron density contours on the mid-plane of the 9x9x9 nano-cluster

Accuracy of subspace projection method commensurate with chemical accuracy

Case study: Alkane chains ($C_{33}H_{68}$– $C_{2350}H_{4702}$)
Pseudopotential calculations

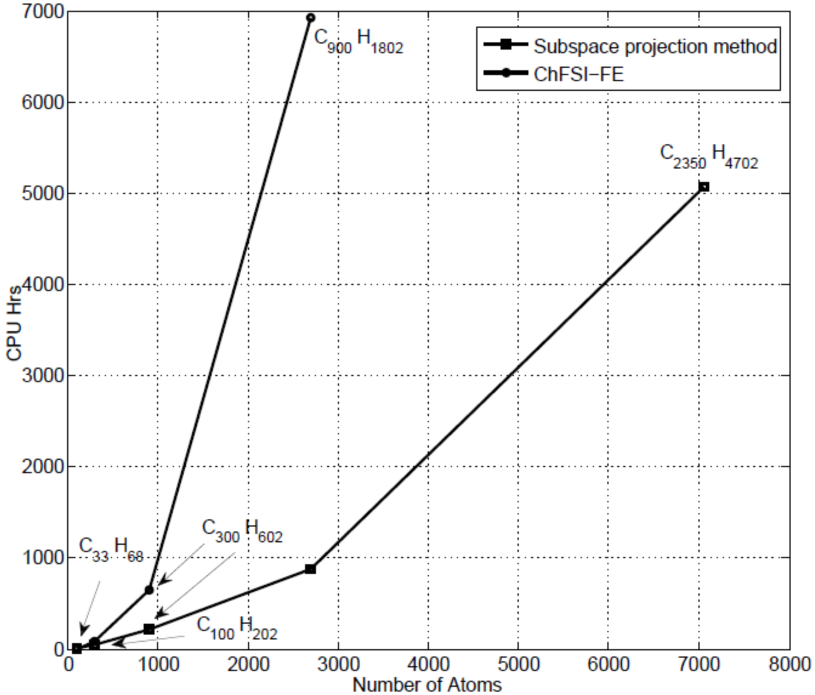

Total computational time

Subspace projection scaling: $O(N^{1.18})$

Numerical accuracy

Alkane Chain	DoF	Proposed Method	ChFSI-FE
C_{33} H_{68}	870, 656	−61.438671	−61.438680
C_{100} H_{202}	2, 491, 616	−62.041530	−62.041532
C_{300} H_{602}	7, 354, 496	−62.240148	−62.240277
C_{900} H_{1802}	21, 943, 138	−62.303101	−62.303608

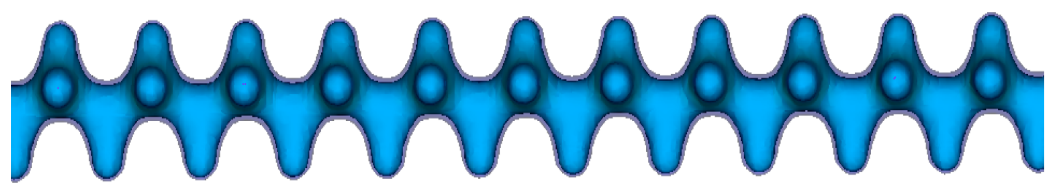

Isocontours of alkane chain $C_{900}H_{1802}$

Case study: Si nano-clusters (1x1x1 – 3x3x3)

All-electron calculations

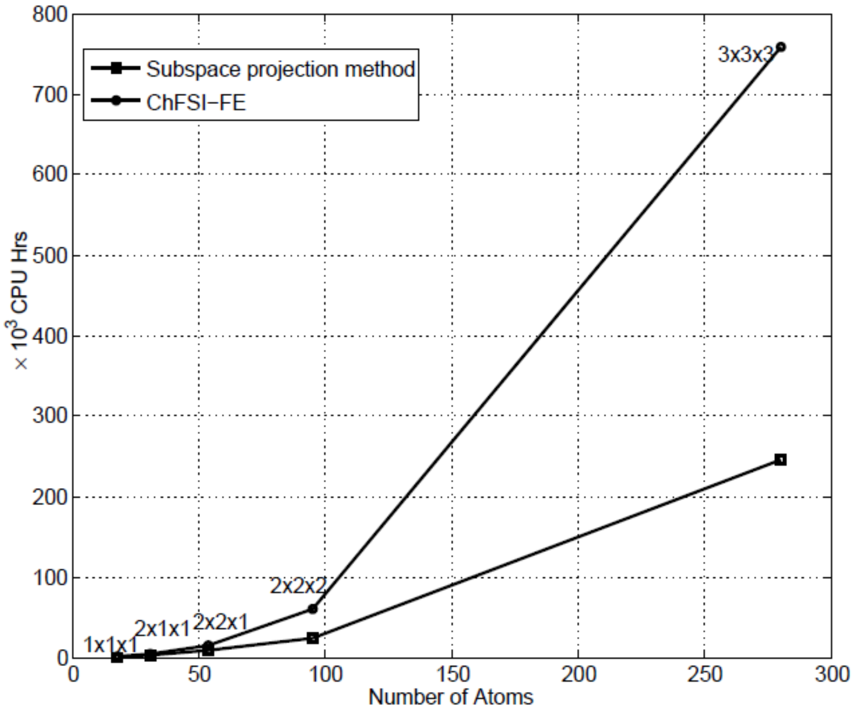

Total computational time

Subspace projection scaling: $O(N^{1.85})$

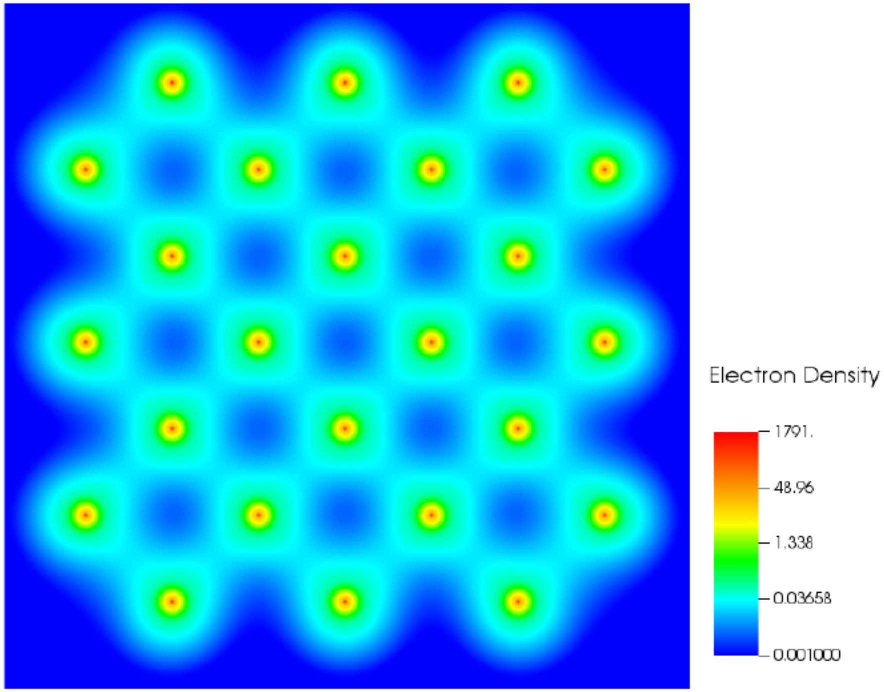

Electron density contours on the mid-plane of the 3x3x3 Si nano-cluster

Accuracy of subspace projection method commensurate with chemical accuracy

Spectrum Splitting: Key ideas

(Motamarri & Gavini et al. Phys. Rev. B 95 035111 (2017))

- The spectral width of subspace projected Hamiltonian grows as $O(Z^2)$
- Split the eigenspectrum of $\tilde{\mathbf{H}}^{\phi}$ into core and valence parts

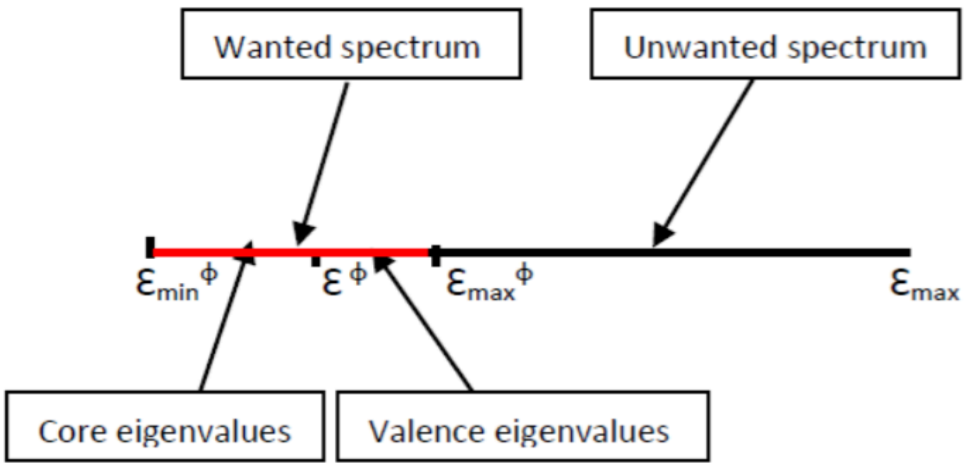

$$\Gamma = \Gamma_{core} + \Gamma_{val}$$

$$\Gamma_{core} = \mathcal{P}^{\phi}_{core} \qquad \Gamma_{val} = f\left((\mathcal{I} - \mathcal{P}^{\phi}_{core})\mathcal{H}^{\phi}(\mathcal{I} - \mathcal{P}^{\phi}_{core})\right)$$

Spectrum Splitting

Case study: Silicon 18 atoms
(1x1x1 nanocluster (252 electrons))

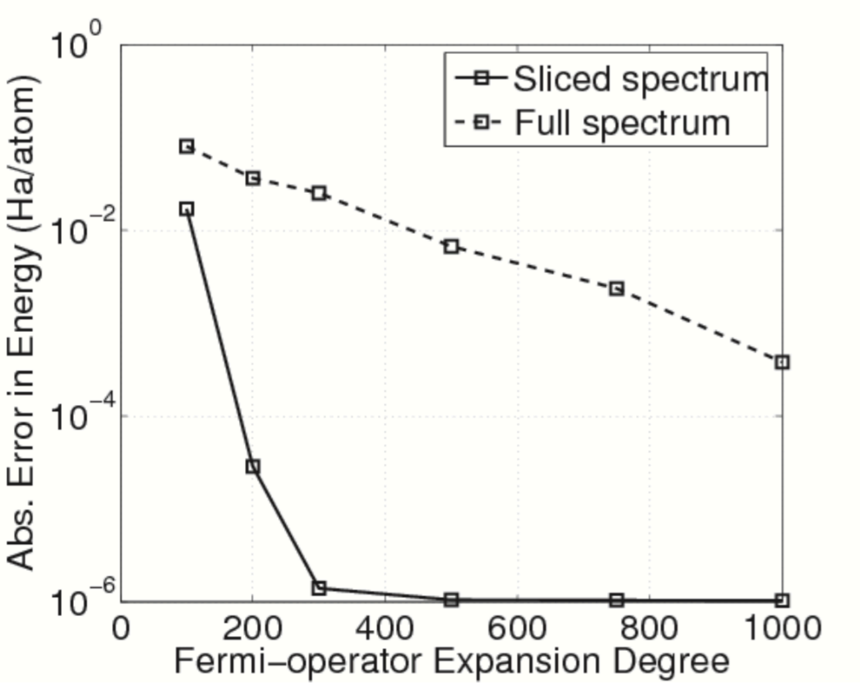

Case study: Silicon 31 atoms
(2x1x1 nanocluster (434 electrons))

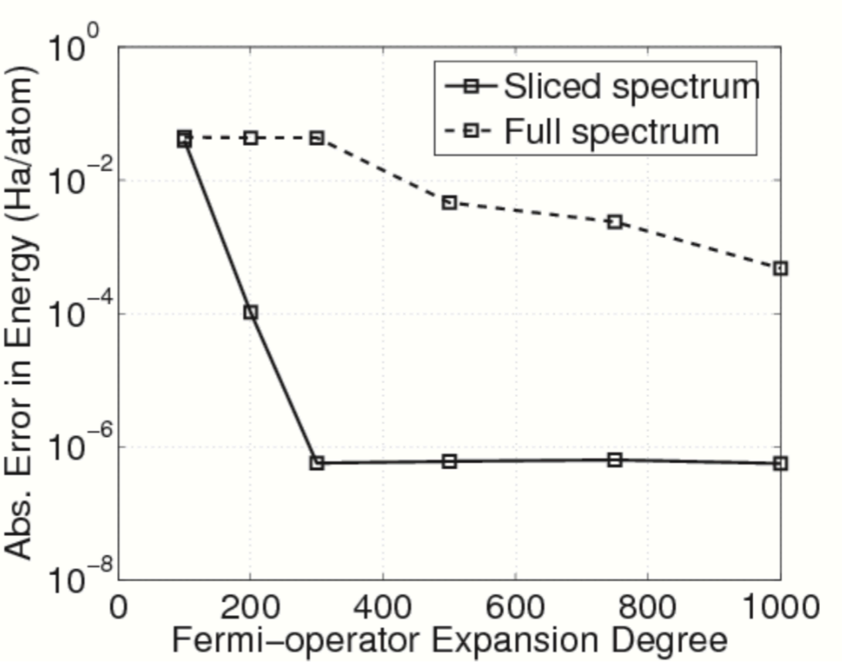

Spectrum Splitting

Case study: Silicon 95 atoms

(2x2x2 nanocluster (1330 electrons))

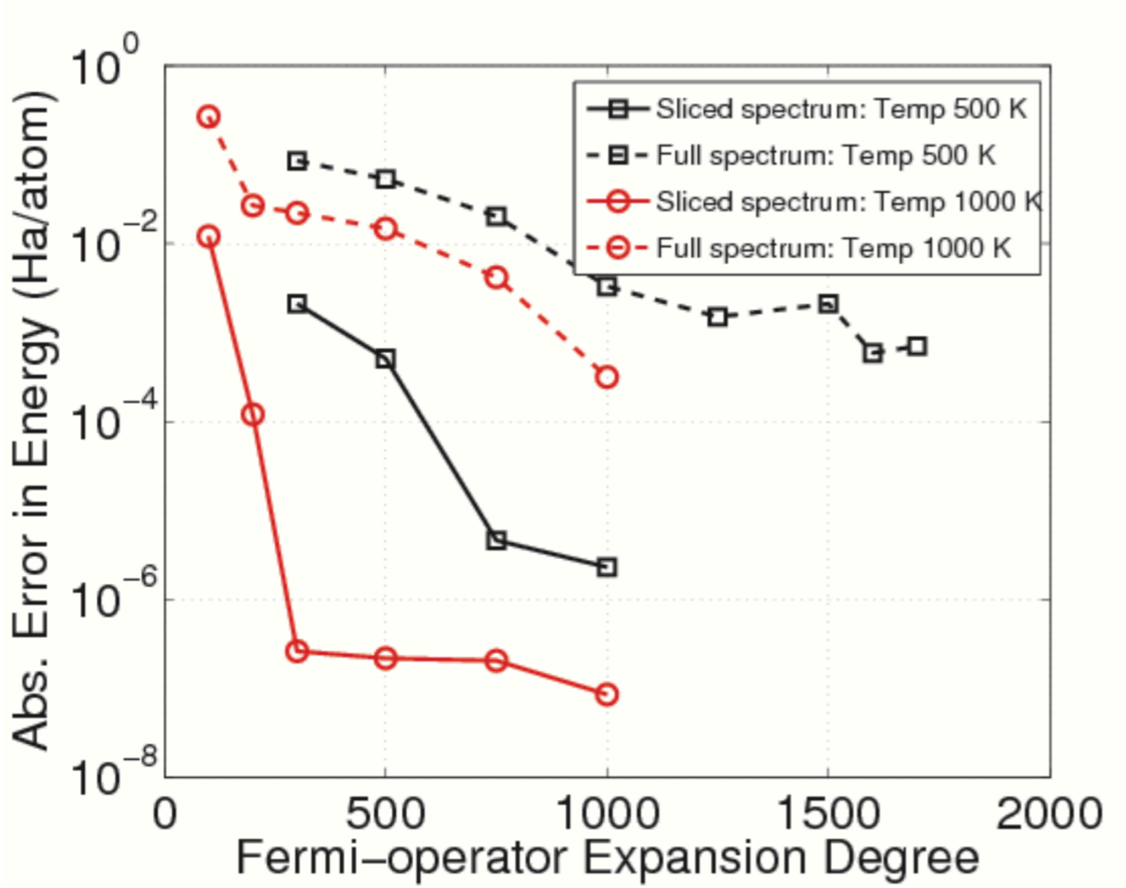

Spectrum Splitting

Case study: Gold Atom
(Single atom (79 electrons))

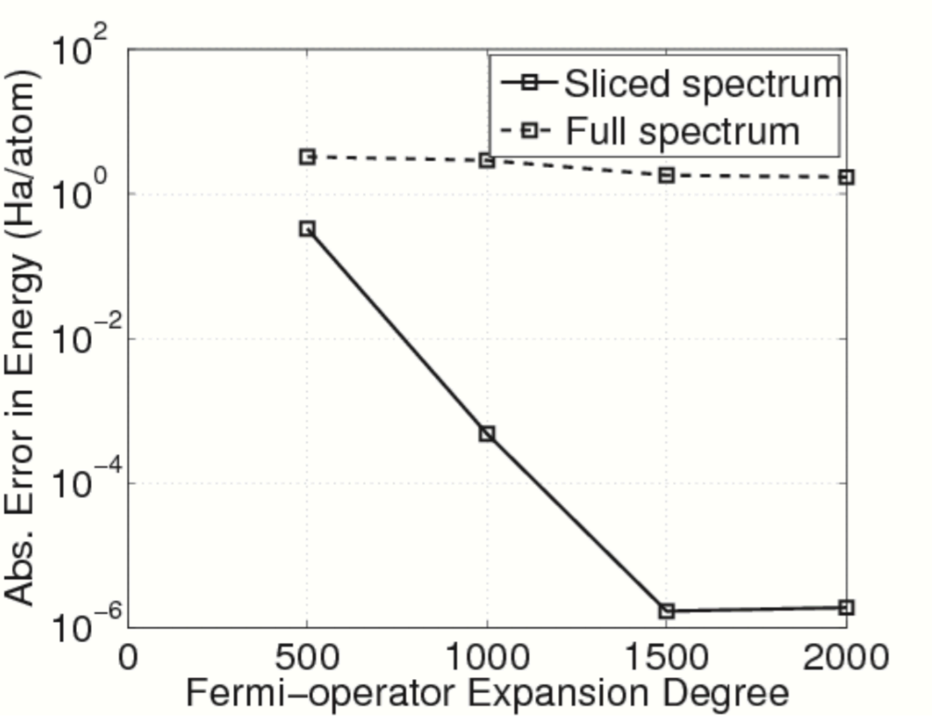

Case study: Gold 6 Atoms
(Nano-cluster (474 electrons))

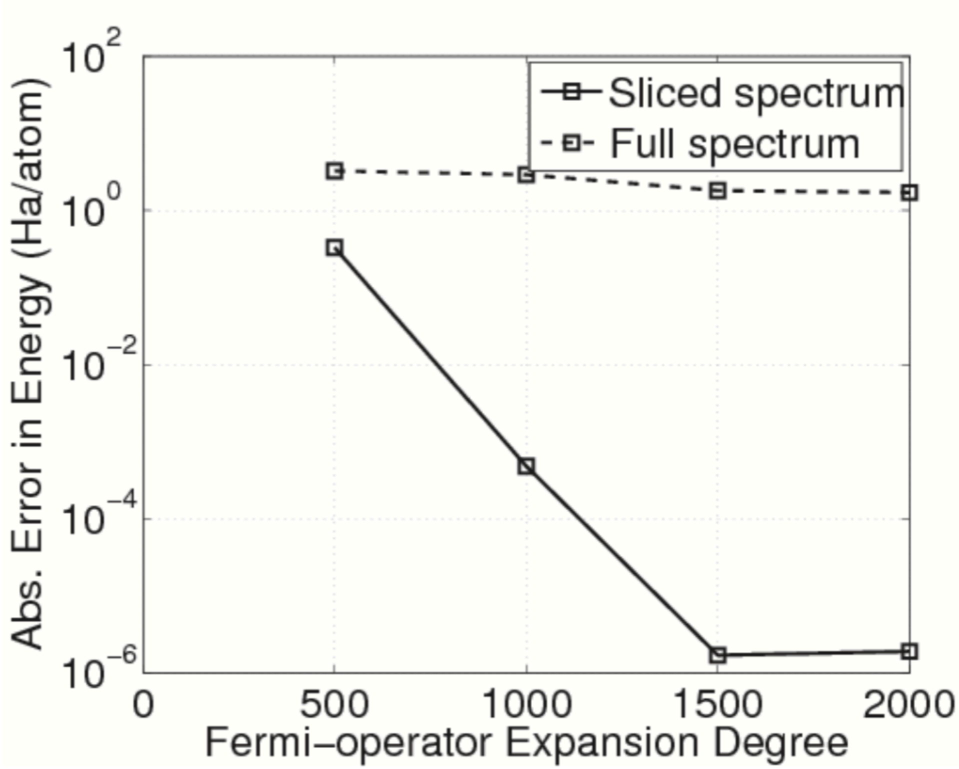

Ongoing/future work

Real-space DFT-FE:

- Incorporate more advanced exchange-correlation functionals (beyond LDA, GGA)
- Exploring tensor structured techniques and low rank approximations in conjunction with real-space formulation

  (Motamarri, P., Blesgen, T., Gavini, V., Tucker-tensor algorithm for large-scale Kohn-Sham density functional theory calculations, Phys. Rev. B, 93 125104 (2016))

- Extend algorithms to time dependent DFT

Coarse-graining KSDFT:

Localization of the wavefunctions is key for extending the coarse-graining ideas

- O(N) formulations: Non-orthogonal localized orbitals
- QC-KSDFT: localization -> predictor-corrector approach -> QC
- Electronic structure calculations at macroscopic scales with Kohn-Sham DFT will enable a quantum-mechanically accurate study of defects in materials

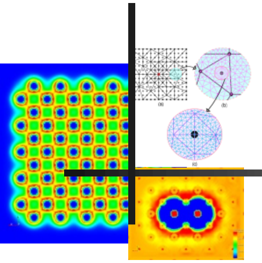

Concluding remarks

- Developed real-space formulation for Kohn-Sham DFT
  - Reformulation of electrostatics as a local variational problem
  - Mathematical analysis

- Finite-element discretization of Kohn-Sham DFT & Numerical algorithms
  - Optimal rates of convergence
  - Spectral elements in conjunction with GLL quadratures (for overlap matrix)
  - Chebyshev filtering to directly compute the eigenspace
  - Large-scale calculations possible
  - Algorithms exhibit good scalability

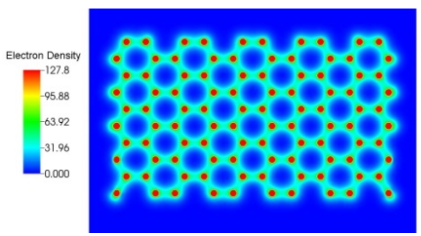

- Development of a linear-scaling algorithm
  - Localized basis spanning the Chebyshev filtered subspace
  - Project of Hamiltonian into subspace
  - Use Fermi-operator expansion on the projected Hamiltonian

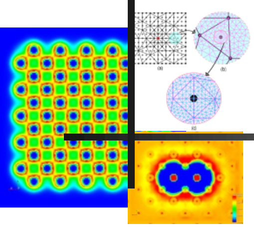

THANK YOU!